Interrogating the Bioactive Pharmacophore of the Latrunculin Chemotype by Investigating the Metabolites of Two Taxonomically Unrelated Sponges

Taro Amagata,[†] Tyler A. Johnson,[†,‡] Robert H. Cichewicz,[†] Karen Tenney,[†] Susan L. Mooberry,[§] Joseph Media,[⊥] Matthew Edelstein,[⊥] Frederick A. Valeriote,[⊥] and Phillip Crews*[,†,‡]

Department of Chemistry and Biochemistry and Department of Ocean Sciences, University of California Santa Cruz, Santa Cruz, California 95064, Southwest Foundation for Biomedical Research, San Antonio, Texas 78245, and Department of Internal Medicine, Division of Hematology and Oncology, Henry Ford Hospital, Detroit, Michigan 48202

Received July 11, 2008

This study involved a campaign to isolate and study additional latrunculin analogues from two taxonomically unrelated sponges, *Cacospongia mycofijiensis* and *Negombata magnifica*. A total of 13 latrunculin analogues were obtained by four different ways, reisolation (**1**−**4**), our repository (**5**, **6**), new derivatives (**7**−**12**), and a synthetic analogue (**7a**). The structures of the new metabolites were elucidated on the basis of a combination of comprehensive 1D and 2D NMR analysis, application of DFT calculations, and the preparation of acetonide derivative **7a**. The cytotoxicities against both murine and human cancer cell lines observed for **1**, **2**, **7**, **7a**, **8**, **9**, and **12** were significant, and the IC_{50} range was 0.5−10 μM. Among the cytotoxic derivatives, compound **9** did not exhibit microfilament-disrupting activity at 5 μM. The implications of this observation and the value of further therapeutic study on key latrunculin derivatives are discussed.

Introduction

The latrunculins are an important group of sponge-derived bioactive small molecules whose properties have been extensively studied for almost 30 years.[1] The two lead compounds of this series are latrunculin A (**1**) and latrunculin B (**2**), originally isolated from the Red Sea sponge *Negombata magnifica* (old genus designation *Latrunculia*).[1,2] Their basic structural motif consists of a macrolide 1,3 fused to a tetrahydropyran containing a 2-thiazolidinone side chain. Compound **1** also shares a carbon skeleton with the anticancer active epothilone A,[3] obtained from cultures of the terrestrial myxobacterium *Sorangium cellulosum*.[4,5] The sustained attention given to the latrunculins can be attributed to three factors: a unique mixed biogenesis from PKS/NRPS,[a,3] their potent actin inhibition properties,[2,6] and their potent cytotoxicity against cancer cell lines.[7] In comparison to the many other common natural product actin inhibitors[8] latrunculin A is the most widely used small molecule molecular probe. Its actin inhibition properties result from blocking the hyperassembly of G-actin to F-actin[6] by binding to a site in a cleft between subdomains II and IV.[9,10]

Somewhat surprising is that little side-by-side experimental therapeutic studies have been conducted on **1**, **2**, and their analogues. In principle, these compounds are available from total syntheses,[11−16] but such a pipeline has not been tapped. Few commercially available compound libraries have entities beyond **1** and **2**. Alternatively, it is possible to encounter these compounds in nature, but the sources are restricted to the marine realm. This project was designed to further probe the biological activity properties of the latrunculin chemotype. Thus, the goals were to reisolate **1** and **2**, obtain new analogues as a minilibrary, and then evaluate them for their antiactin and cancer cell line cytoxicity activities. Another goal was to use the isolation results to gain a better understanding of chemical ecology of both *N. magnifica* and *C. mycofijiensis* that are both reliable sources of these compounds. We believed this could be accomplished by examining selected collections housed in our repository.

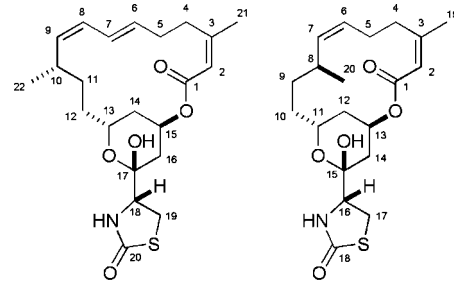

1 **2**

Results and Discussion

Initially, the experimental design used in this study was influenced by insights obtained from evaluating literature to assess the breadth of latrunculin analogues isolated according to their source organisms. Prior to our work outlined below, a total of 13 latrunculin family compounds had been reported, headed by **1**, **2**, and 11 analogues. Collectively, this information assembled in Table 1 (the entire list is shown in Table S1 of Supporting Information) indicated that there was a diverse group of sponges as sources of these compounds. This data set contains the sponge taxonomic identification reported, the collection location, and the latrunculin frameworks observed among the isolated metabolites. There is no biological crossover between the occurrences of Red Sea sponges versus those from the Indo Pacific. Alternatively, with only one exception, **1** has been

* To whom correspondence should be addressed. Tel: (831) 459-2603. Fax: (831) 459-4197. Email: phil@chemistry.ucsc.edu.

† Department of Chemistry and Biochemistry, University of California—Santa Cruz.

‡ Department of Ocean Sciences, University of California—Santa Cruz.

§ Southwest Foundation for Biomedical Research.

⊥ Henry Ford Hospital.

[a] Abbreviations: DFT, density functional theory; PKS/NRPS, polyketide synthase/nonribosomal peptide synthetase; MAE, mean absolute error; colon 38, murine colon adenocarcinoma; L1210, murine lymphocytic leukemia; CFU-GM, murine bone marrow; HCT-116, human colorectal carcinoma; MDA-MB-435, human breast cancer; SRB, sulforhodamine B; A10, rat smooth muscle; DTP, developmental therapeutics program.

10.1021/jm8008585 CCC: $40.75
Published on Web 10/23/2008

Table 1. Summary of Latrunculin Frameworks and Their Biological Sources[a]

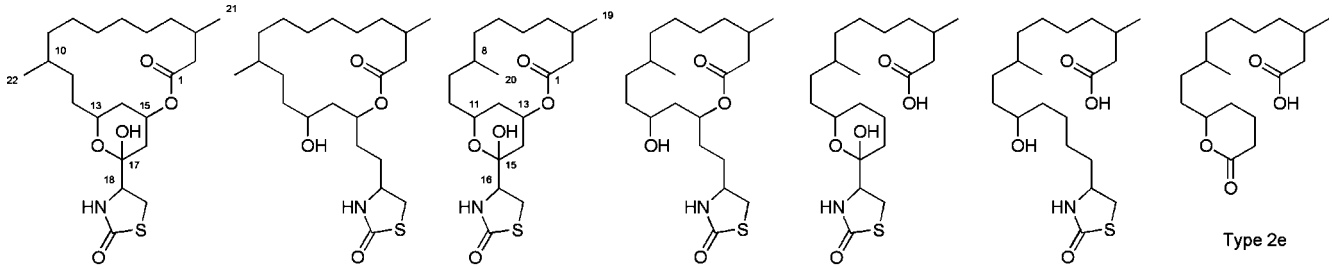

		type 1			type 2			
taxonomic identification	collection site	1a	1b	2a	2b	2c	2d	2e
		Group A						
Negombata magnifica	Dahlak Archipelago	x						
	Djibouti	x		x				
	Egypt	x		x			x	
	Israel			x	x			x
	Tiran Straits	x		x			x	
	not specified	x				x		
N. corticata	Egypt			x				
		Group B						
Cacospongia mycofijiensis	Fiji	x						
	Indonesia	x						
	Marshall Islands	x						
	Papua New Guinea	x						
	Solomon Islands	x						
	Tonga	x						
	Vanuatu	x						
		Group C						
Dactylospongia sp.	Vanuatu	x						
Fasciospongia rimosa	Okinawa	x	x					
Hyattella sp.	Indonesia	x						
unidentifiable	American Samoa	x						

[a] The entire list including cited literature is in Table S1.

observed from all of the organisms listed. There are two main carbon frameworks present in these compounds: octaketide containing (type 1) and heptaketide containing (type 2). These can be further subdivided into the six distinct architectures based on the count of rings that are present: three (type 1a or 2a), two (type 1b, 2b, or 2c), or one (types 2d and 2e). There are two other significant structural features present among all the latrunculin family frameworks; all have *S* chirality at the carbon bearing the methyl group most distant from the ester carbonyl, and the relative orientations of all three of the tetrahydropyran ring substituents are conserved. Other noteworthy chemical ecology patterns include the following: (a) The taxonomically unrelated sponges in groups A and B, briefly noted above as *N. magnifica*[2] and *C. mycofijiensis,*[17] are a reliable source of latrunculin A. (b) We believe three sponges of group C, *Dactylospongia*, *Fasciospongia*, and *Hyattella*, have been misidentified, and (c) one sponge of group C was not identified. In summary, the significant chemical ecology insights based in Table 1 suggested that the most direct route to obtain a diverse minilibrary of latrunculin frameworks would be through re-examination of *Negombata* specimens. Also, an extensive evaluation of *Cacospongia* collections was initially thought to be less useful because of their narrow chemical diversity as shown in Table 1.

The observations outlined above dictated that the initial investigation begin on Red Sea derived *N. magnifica*. Isolation work on a collection obtained in 2001 eventually afforded three known compounds: **2**,[1] 16-*epi*-latrunculin B (**3**),[8] and latrunculin C (**4**)[18] (Chart S1 of Supporting Information). An additional two compounds were added to this cache from our previous study of a 1988 collection of this species. These included the known 15-methoxylatrunculin B (**5**) and one new analogue at the point of publication, latrunculeic acid (**6**).[19] Overall, these provided examples of the three of the six frameworks expected, including compounds of types 2a, 2b, and 2e.

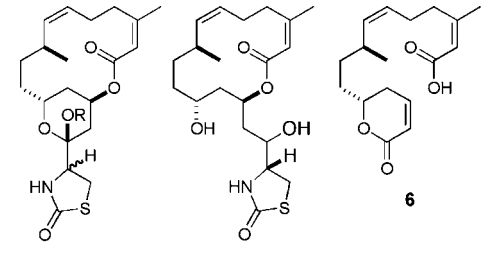

It appeared, on the basis of the LCMS results (data not provided) of the crude extracts, that the only possibility for isolating additional chemotypes from *Cacospongia mycofijiensis* would occur through the investigation of minor components. This effort was begun with the large Fijian samples collected in 1989 and 2000. Surprisingly, the 1989 collection (5.8 kg) was devoid of **1** but was a source for mycothiazole[20] and CTP-431[21] whose polyketide skeleton was closely related to that of **1**, plus minor amounts of new latrunculin derivatives that were not characterized. The isolation results for the 2000 collection [collection numbers 00100-I and -II (1.9 and 0.6 kg)] were much

more rewarding as eight compounds were obtained. The extraction method was the same as that described above, and the resultant CH_2Cl_2 extract purified by reversed-phase HPLC (Chart S2) afforded **1** and **2**, plus new analogues latrunculol A (**7**), latrunculol B (**8**), 18-*epi*-latrunculol A (**9**), latrunculol C (**10**), latrunculone A (**11**), and latrunculone B (**12**). These compounds, which are type 1a frameworks (Table 1), were valuable additions because they possessed highly modified macrocyclic rings. The known latrunculins isolated from the *Negombata* and *Cacospongia* sponges were identified by comparison of their ^{1}H and ^{13}C NMR data to those of published values. The data in support of structure shown for the six new entities follow next.

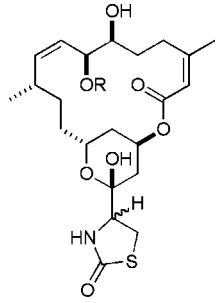

7: R = H, 18*R*
8: R = CH_3, 18*R*
9: R = H, 18*S*

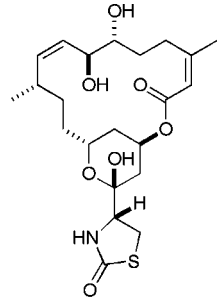

10

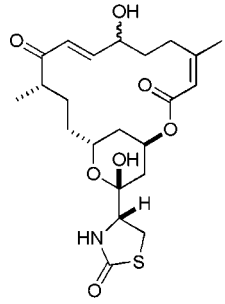

11

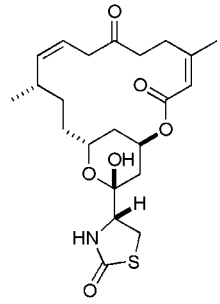

12

The elucidation of the planar structure for **7** was performed in a succinct manner once its molecular formula was established by HRESIMS as $C_{22}H_{33}NO_7S$. Relative to **1** there were two additional H and O atoms each and one less unsaturation equivalent. The diene chromophore of **1** was now present in **7** as a monoene diol, which was substantiated from the NMR data. The ^{1}H and ^{13}C NMR spectra of **7** revealed that, vs **1**, signals of the Δ^6 double bond of **1** were replaced by two oximethine signals (Tables 2 and 3) for a vicinal diol. Though the $^3J_{6,7}$ was not detectable, mutual gCOSY correlations were observed (Table S6). As expected, the remaining functional groups included (1) a thiazolidinone carbonyl [δ 173.9 (C-20)], (2) an ester carbonyl [δ 166.6 (C-1)], (3) a disubstituted double bond [δ 5.64 (H-8), 5.05 (H-9), δ 132.3 (C-8), 136.5 (C-9)], (4) a trisubstituted double bond [δ 5.54 (H-2), δ 118.7 (C-2), 158.3 (C-3)], and (5) a hemiacetal quaternary carbon [δ 97.6 (C-17)]; all were consistent with the type 1a system. Finally, the COSY and HMBC NMR data further substantiated (Table S6) the proposed planar structure of **7**.

Unraveling all the absolute stereochemical elements of **7** proved to be challenging. Establishing the spatial relationship between the three tetrahydropyran ring substituents plus that at C-18 was not the problem. These were readily determined from ^{1}H NMR coupling constant magnitudes. The large and small J values between H-13 and H-14a (J = 11.3 Hz), H-13 and H-14b (J = 3.8 Hz), and H-15 and H_2-16 ($J_{15,16a}$ = 4.3 and $J_{15,16b}$ = 2.0 Hz) mirrored that of **1**. Clearly, two of the groups appended to the chair conformation pyran ring consisted of an equatorial C-13−C-12 bond and an axial C-15−O, possessing 13*R**, 15*R** configurations. The C-17 and C-18 chirality was deduced to be 17*R** and 18*R** because of the parallel NMR data of **7** [δ 97.6 (C-17), δ 3.86, ddd, J = 8.6, 6.5, and 1.2 Hz (H-18), δ 63.4 (C-18)] versus **1** [δ 96.9 (C-17), δ 3.87, dd, J = 8 and 7 Hz (H-18), δ 62.1(C-18)][22] with *R* configuration at these sites. Next, the C-7 and C-10 centers were deduced to be 7*S** and 10*S**, as a strong NOE correlation was observed between H-7 and H-10. The additional NOE correlation observed between H-10 and H-13 made it possible to further interrelate all three as 7*S**, 10*S**, and 13*R**. (Table S6). Tying in the relative stereochemistry at C-6 was accomplished through the NMR analysis of the acetonide **7a** obtained from **7** by treatment with 2,2-dimethoxypropane and pyridinium *p*-toluene sulfonate. The relatively large coupling constant of **7a** between H-6 and H-7 ($J_{6,7}$ = 8.6 Hz) and the NOEs observed from H-6 to H-8 and H-7 to H-10 as shown in Figure 1 all suggested a 6,7-anti configuration.[23] Therefore, the stereochemistry of H-6 was determined to be 6*S** building on the 7*S** assignment.

Converting the relative assignments enumerated above into absolute stereochemical designations was accomplished by examining the sensitivity of ^{13}C δ values to changes in the C-6 and C-7 configurations. Such analysis for **7** was launched through DFT calculations, which involved comparing the experimental data to ^{13}C chemical shifts calculated for four possible diastereomers based on chirality changes at these two sites. The software Spartan 06 was employed and primed with the dual basis sets, B3LYP/6-31G*//B3LYP/6-31G* level.[24] We have previously demonstrated the power of the preceding basis sets as a calculation tool and have defined the empirically derived expectation for acceptable agreement (experimental vs calculated) assessed by an MAE of <2.2, and a % Score of >85.[25] The best agreement among the four diastereomers of **7** shown in Table 4 (and Tables S12−S15 of Supporting Information) was observed for the 6*S*, 7*S* isomer with % Score = 95 and MAE = 2.1. Thus, the final assignments for **7** consist of 6*S*, 7*S*, 10*S*, 13*R*, 15*R*, 17*R*, 18*R*. These match those at the biosynthetically common chiral centers of **1** (at C-10, C-13, C-15, C-17, and C-18) whose absolute stereostructure has been unambiguously determined.[26]

The compounds **8**, **9**, and **10** were close in structure to **7**, and this simplified their characterizations. Compound **8** of $C_{23}H_{35}NO_7S$ had an extra CH_2 compared to that of **7**, which was assigned as a methoxyl group (δ_H 3.24, s, δ_C 56.5). The ^{13}C NMR signal (Tables 2 and 3) at C-7 in **8** was shifted upfield by 9 ppm vs that of **7**, making the point of attachment for the OCH_3 group obvious, which was further confirmed by the 2D NMR data (Table S7). Parallel absolute chirality between **8** and **7** was proposed on the basis of the nearly identical ^{1}H J values and ^{13}C δs values at each chiral center. Compounds **9** ($C_{22}H_{33}NO_7S$) and **10** ($C_{22}H_{33}NO_7S$) were each diastereoisomers of **7** because each of the trio exhibited nearly similar ^{1}H and ^{13}C NMR properties (Tables S8 and S9 of Supporting Information). A minute, but distinct, difference between **9** and **7** was in the coupling constant patterns to H-18 (**9**, 3.92 td, J = 8.1 and 1.2 Hz; **7**, 3.86, ddd, J = 8.6, 6.5 and 1.2 Hz). Therefore, compound **9** was designated as 18-*epi*-latrunculol A. Additional support for this conclusion came by noting the ^{1}H NMR data at H-18 in **9** were parallel to that of the isostructural 16*S* proton

Table 2. ^{1}H NMR Data for **7**−**12** (600 MHz)

	δ_H (mult, J in Hz)					
position	**7**[a]	**8**[a]	**9**[a]	**10**[a]	**11**[a]	**12**[b]
2	5.54 (q, 1.0)	5.55 (q, 1.0)	5.56 (q, 1.2)	5.63 (q, 1.0)	5.59 (q, 1.2)	5.69 (q, 1.2)
4a	2.58 (td, 11.6, 5.4)	2.54 (td, 11.4, 5.4)	2.57 (td, 11.5, 5.3)	2.59 (ddd, 13.4, 10.4, 6.3)	2.35 (td, 12.0, 5.3)	2.26 (ddd, 13.2, 8.4, 6.0)
4b	2.63 (td, 11.6, 5.2)	2.66 (td, 11.4, 5.2)	2.69 (td, 11.5, 5.0)	3.34 (ddd, 13.4, 10.3, 5.2)	2.96 (td, 12.0, 6.2)	3.29 (ddd, 13.2, 9.0, 7.2)
5a	1.82 (m)	1.81 (m)	1.81 (m)	1.84 (m)	1.84 (2H, m)	2.61 (ddd, 15.6, 9.0, 7.2)
5b	1.88 (m)	1.86 (m)	1.88 (m)	1.94 (m)		2.73 (ddd, 14.4, 8.4, 6.0)
6	3.36 (dd, 8.9, 4.5, 1.5)	3.34 (br s)	3.38 (ddd, 9.1, 4.5, 1.5)	3.53 (ddd, 8.2, 5.0, 3.1)	4.31 (td, 8.4, 4.1)	
7a	4.34 (d, 9.6)	3.99 (d, 9.8)	4.37 (d, 9.6)	4.26 (t, 8.4)	7.03 (dd, 16.3, 8.6)	2.96 (ddd, 17.4, 6.6, 1.8)
7b						3.35 (ddd, 17.2, 6.2, 1.1)
8	5.64 (t, 10.3)	5.57 (t, 10.3)	5.65 (t, 10.3)	5.35 (dd, 11.0, 8.6)	5.96 (d, 16.1)	5.45 (dddd, 10.8, 9.6, 6.6, 0.6)
9	5.05 (td, 10.9, 1.0)	5.33 (td, 10.9, 1.0)	5.07 (td, 10.9, 1.0)	5.21 (t, 11.0)		5.33 (m)
10	2.73 (m)	2.81 (m)	2.78 (m)	2.68 (m)	3.69 (m)	2.40 (m)
11a	1.06 (ddt, 13.7, 11.5, 4.0)	1.10 (ddt, 13.7, 11.4, 3.8)	1.07 (ddt, 13.6, 11.5, 4.0)	1.13 (m)	1.60 (dddd, 13.2, 11.5, 4.8, 3.1)	1.16 (dddd, 13.6, 9.5, 5.7, 3.3)
11b	1.89 (m)	1.93 (m)	1.96 (m)	1.55 (m)	1.82 (m)	1.66 (m)
12a	1.45 (2H, m)	1.47 (2H, m)	1.47 (2H, m)	1.54 (2H, m)	1.29 (dddd, 14.2, 12.5, 4.8, 3.4)	1.48 (2H, m)
12b					1.42 (dddd, 14.2, 11.5, 4.3, 3.0)	
13	4.29 (tdd, 11.3, 3.8, 1.9)	4.29 (tdd, 11.3, 3.8, 1.9)	4.33 (tdd, 11.3, 3.6, 2.1)	4.57 (m)	4.35 (dt, 11.6, 2.8)	3.88 (tdd, 10.2, 4.2, 2.4)
14a	1.59 (ddd, 14.7, 11.3, 3.8)	1.60 (ddd, 14.8, 11.3, 3.8)	1.61 (ddd, 14.8, 11.3, 3.6)	1.52 (ddd, 14.4, 7.8, 2.9)	1.53 (ddd, 14.6, 11.6, 3.4)	1.42 (ddd, 15.0, 12.0, 3.0)
14b	1.80 (m)	1.83 (m)	1.82 (m)	2.04 (m)	1.65 (ddd, 14.4, 4.8, 2.1)	2.02 (m)
15	5.19 (m)	5.21 (m)	5.16 (m)	5.29 (m)	5.30 (m)	5.33 (m)
16a	1.81 (dd, 14.9, 4.3)	1.84 (dd, 14.9, 4.3)	1.79 (dd, 14.9, 4.2)	1.88 (dd, 14.6, 4.1)	1.86 (dd, 15.1, 4.3)	1.92 (dt, 14.4, 3.6)
16b	2.25 (dt, 14.9, 2.0)	2.26 (dt, 14.9, 2.0)	2.17 (dt, 14.9, 2.0)	2.14 (dt, 14.6, 2.1)	2.15 (dt, 15.1, 2.2)	2.08 (dt, 14.4, 1.8)
18	3.86 (ddd, 8.6, 6.5, 1.2)	3.86 (ddd, 8.6, 6.5, 1.2)	3.92 (td, 8.1, 1.2)	3.87 (ddd, 8.9, 6.5, 1.2)	3.91 (ddd, 8.8, 6.5, 1.2)	3.82 (ddd, 9.0, 6.0, 1.2)
19a	3.45 (dd, 11.5, 8.6)	3.45 (dd, 11.5, 8.6)	3.43 (dd, 11.2, 7.7)	3.44 (dd, 11.5, 8.9)	3.47 (dd, 11.5, 8.7)	3.41 (dd, 11.4, 6.0)
19b	3.48 (dd, 11.5, 6.5)	3.48 (dd, 11.5, 6.5)	3.45 (dd, 11.2, 8.1)	3.48 (dd, 11.5, 6.3)	3.51 (dd, 11.5, 6.3)	3.48 (dd, 11.4, 9.0)
21	1.90 (d, 1.5)	1.92 (d, 1.5)	1.92 (d, 1.5)	1.92 (d, 1.2)	1.92 (d, 1.5)	1.90 (d, 1.2)
22	0.92 (d, 6.5)	0.97 (d, 6.5)	0.94 (d, 6.7)	0.94 (d, 6.4)	0.99 (d, 6.9)	0.94 (d, 6.6)
NH	7.04 (br s)	7.05 (br s)	6.58 (br s)	6.97 (br s)	7.13 (br s)	5.71 (br s)
6-OH	4.83 (br s)	3.12 (br s)	nd[c]	3.22[c] (br s)	5.12[c] (br s)	
7-OH	3.59[c] (br s)		nd[c]	3.75[c] (br s)		
17-OH	nd[c]	4.84 (br s)	nd[c]	4.78[c]	nd[c] (br s)	nd[c]
7-OCH_3		3.24 (s)				

[a] Measured in acetone-d_6. [b] Measured in $CDCl_3$. [c] Assignments may be switched. nd = not detected.

Table 3. ^{13}C NMR Data for **7**−**12** (125 MHz)

	δ_C (type)					
position	**7**[a]	**8**[a]	**9**[a]	**10**[a]	**11**[a]	**12**[b]
1	166.6 (C)	167 (C)	166.8 (C)	166.6 (C)	166.6 (C)	165.4 (C)
2	118.7 (CH)	119 (CH)	118.7 (CH)	118.7 (CH)	119.5 (CH)	118.0 (CH)
3	158.3 (C)	159 (C)	158.7 (C)	159.5 (C)	156.9 (C)	156.3 (C)
4	32.2 (CH_2)	32.5 (CH_2)	31.9 (CH_2)	27.3 (CH_2)	29.4[c] (CH_2)	27.7 (CH_2)
5	35.4 (CH_2)	35.9 (CH_2)	33.2 (CH_2)	30.3[c] (CH_2)	35.6 (CH_2)	41.0 (CH_2)
6	76.6 (CH)	76.5 (CH)	76.7 (CH)	73.4 (CH)	73.5 (CH)	207.4 (C)
7	70.1 (CH)	79.6 (CH)	70.2 (CH)	70.0 (CH)	149.6 (CH)	41.5 (CH_2)
8	132.3 (CH)	129 (CH)	132.4 (CH)	131.4 (CH)	132.0 (CH)	119.7 (CH)
9	136.5 (CH)	140 (CH)	136.7 (CH)	139.2 (CH)	205.9[d] (C)	140.0 (CH)
10	29.3 (CH)	29.8[c] (CH)	29.9[c] (CH)	29.9[c] (CH)	36.4 (CH)	29.0 (CH)
11	32.0 (CH_2)	31.9 (CH_2)	32.2 (CH_2)	32.1 (CH_2)	29.4 (CH_2)	31.0 (CH_2)
12	32.9 (CH_2)	32.9 (CH_2)	35.4 (CH_2)	31.7 (CH_2)	32.4[c] (CH_2)	31.9 (CH_2)
13	62.3 (CH)	62.3 (CH)	62.6 (CH)	63.8 (CH)	63.1 (CH)	62.5 (CH)
14	36.6 (CH_2)	36.6 (CH_2)	36.9 (CH_2)	35.2 (CH_2)	36.3 (CH_2)	34.6 (CH_2)
15	68.2 (CH)	68.2 (CH)	68.1 (CH)	68.3 (CH)	67.9 (CH)	68.4 (CH)
16	32.0 (CH_2)	32.0 (CH_2)	32.6 (CH_2)	32.2 (CH_2)	36.5 (CH_2)	31.3 (CH_2)
17	97.6 (C)	97.7 (C)	97.4 (C)	98.1 (C)	97.7 (C)	97.3 (C)
18	63.4 (CH)	63.5 (CH)	64.0 (CH)	63.5 (CH)	63.6 (CH)	61.5 (CH)
19	28.9[c] (CH_2)	29.0[c] (CH_2)	29.4[c] (CH_2)	29.1[c] (CH_2)	29.0[c] (CH_2)	28.7 (CH_2)
20	173.9 (C)	174.0 (C)	174.2 (C)	173.9[d] (C)	174.0 (C)	174.9 (C)
21	25.4 (CH_3)	25.5 (CH_3)	25.5 (CH_3)	24.6 (CH_3)	25.1 (CH_3)	24.7 (CH_3)
22	23.1 (CH_3)	23.0 (CH_3)	23.2 (CH_3)	21.4 (CH_3)	19.6 (CH_3)	21.5 (CH_3)
OCH_3		56.5 (CH_3)				

[a] Measured in acetone-d_6. [b] Measured in $CDCl_3$. [c] Assignments from HMQC correlations (the spectra of **7**−**11** are available in Figures S11, S14, S17, S20, and S23, respectively), [d] Assignments from HMBC correlations (the spectra of **10** and **11** are available in Figures S21 and S25).

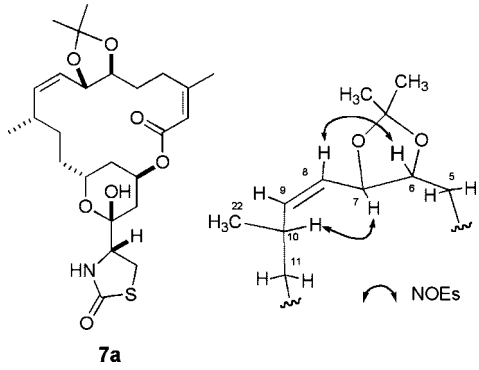

Figure 1. Structure of acetonide **7a** and its key NOEs.

Table 4. DFT Calculation Results of the Possible Isomers for **7** and **10**

	7		**10**	
stereochemistry	% Score	MAE (ppm)	% Score	MAE (ppm)
6*S*,7*S*	95	2.1	86	2.1
6*R*,7*S*	95	2.4	95	1.7
6*S*,7*R*	86	2.6	77	3.0
6*R*,7*R*	86	2.5	86	2.2

of **3** (δ 3.87 ddd, J = 8.5, 8.5, and 1.0 Hz).[8] Thus, on the basis of this consideration and in analogy to **1**, the absolute chirality of **9** was deduced as 6*S*, 7*S*, 10*S*, 13*R*, 15*R*, 17*R*, 18*S*. The last compound **10** was concluded to have identical relative configurations at C-17 and C-18 compared to **1** and **7** because of congruence of the NMR data at these sites. In addition, NOEs (Table S9) between (a) H-10 and H-7, (b) H-13 and H-7, (c) H-13 and H-10, plus the diagnostic J values to H-15 enabled assignment of the 7*S**, 10*S**, 13*R**, 15*R** configurations for **10**. Lastly, C-6 must be 6*R** to render **10** isomeric to **7**. To confirm this conclusion, the DFT calculated vs experimental ^{13}C shifts obtained for the four C-6 and C-7 diastereormers of **10** were analyzed as shown in Table 4. The best fit was for 6*R*,7*S*, which gave % Score = 95 and MAE = 1.7 (Table 4 and Tables S16−S19). With this last assignment completed and by biogenetic analogy to the configurations in **1**, the absolute structure of latrunculol C was deduced to be 6*R*, 7*S*, 10*S*, 13*R*, 15*R*, 17*R*, 18*S*.

The last compounds to be characterized were **11** of $C_{22}H_{31}NO_7S$ and **12** of $C_{22}H_{31}NO_6S$, whose formulas were established from the HRESIMS data. The low field ^{13}C δ values clarified that both possessed ketone residues. The allylic alcohol in **7** was replaced by a *trans*-enone in **11** recognized by signals at δ 205.9 (C-9) and δ 7.03 dd, J = 16.3 and 8.6 Hz, (H-7), δ 5.96, d, J = 16.1 Hz (H-8), δ 149.6 (C-7), δ 132.0 (C-8). The planar structure of **11** (Table S9) was finalized by observing key HMBC correlations (H-22/C-9, H-8/C-10, and H-7/C-9) and key COSY correlations (H-6/H-7 and H-7/H-8). The geometry of the trans double bond at C-7−C-8 was also determined on the basis of 1D NOESY correlations from H-6 to H-8, from H-7 to H-10, and from H-13 to H-7. The NMR data of **12** indicated a homo conjugated *trans*-enone [δ 207.4 (C-6)] with a clearly visible bis-allylic methylene group [δ 2.96 and 3.35 (H_2-7), δ 41.5(C-7)]. The key COSY correlations (H-5/H-6 and H_2-7/H-8 and H-8/H-9) and HMBC correlations (H-5/C-6 and H-8/C-6) signified the planar structure **12**. The absolute configurations for **11** at the tetrahydropyrane and the thiazolidinone rings were deduced to be the same as those in **7**, **8**, and **10** because of the similar proton and carbon NMR profiles at each of pertinent chiral centers. The 10*S* configuration was based on analogy to that of the latrunculin A congeners, but none of the data collected allowed definition of the stereochemistry at C-6. The absolute structure of **12** was provisionally assigned 10*S*, 13*R*, 15*R*, 17*R*, 18*R* based on its biogenetic relationship to **l**.

A minilibrary of 13 compounds was obtained in sufficient quantity to engage in bioactivity assessment. This included 10 metabolites (**1**−**4**, **7**−**12**) isolated in this study, two latrunculin analogues (**5**, **6**) from our pure compound repository, and the synthetic derivative **7a**. Each was evaluated in the disk diffusion soft agar cell-based assay against murine cell lines shown in Figure 2: colon 38, L1210, and CFU-GM.[27] Compounds were adsorbed onto the disk at similar concentrations, and a zone of inhibition (Z) in mm was recorded. Somewhat surprisingly, one

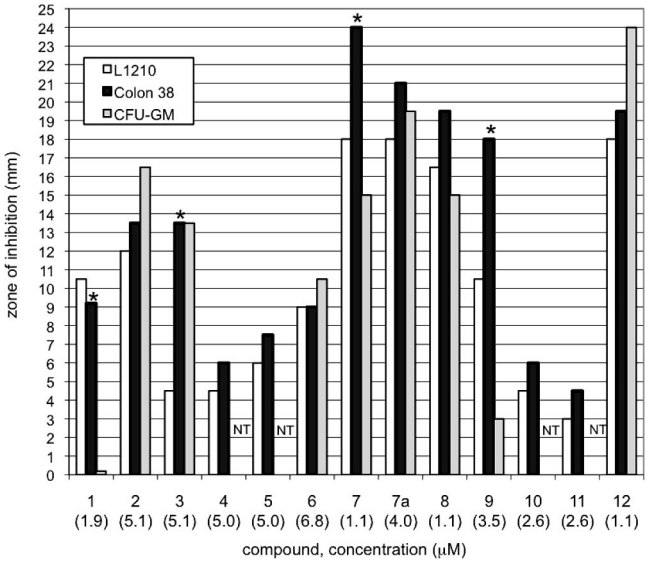

Figure 2. Cytotoxicity against murine cell lines for **1**−**12** and **7a**: (∗) selective cytotoxicity (>7.5 mm difference) for murine cell lines L1210, colon 38, CFU-GM. Each compound was applied onto a disk with 15 μL of DMSO solution of the concentration given in the figure. NT = not tested. DMSO used as a control showed no ctotoxicity against all the cell lines (zone inhibition = 0 mm).

of the new compounds, **7**, showed the best cytotoxic effect against colon 38 (Z_{C38} = 23.5 mm at 1.1 μM), which was 2.6 and 1.8 times greater than **1** (Z_{C38} = 9.0 mm at 1.9 μM) and **2** (Z_{C38} = 13.0 mm at 5.1 μM), respectively. Four other compounds were almost as effective against colon 38, and these included acetonide **7a** (Z_{C38} = 21.0 mm at 4.0 μM), **8** and **12** (each Z_{C38} = 19.5 mm at 1.1 μM), followed by **9** (Z_{C38} = 17.0 mm at 3.5 μM). Examining the relative sensitivity of the two other cell lines to these and the other compounds provided an assessment of their relative solid tumor selective cytotoxicity.[27] Four compounds fit this designation and are flagged by a an asterisk (∗) in Figure 2. These include **1**, **3**, **7**, and **9** with colon 38 selective in their cytotoxicity effect as follows. The magnitude of the differential selective cytotoxicity for **7** was identical to that of **1** ($Z_{C38} - Z_{CFU\text{-}GM}$ = 9.0 mm). Interestingly, compound **9** ($Z_{C38} - Z_{CFU\text{-}GM}$ = 15.0 mm), the 18*S* epimer of **7**, exhibited the greatest overall differential selective cytotoxicity. A similar enhancement of relative solid tumor selectivity was also seen when comparing the epimers **3** ($Z_{C38} - Z_{L1210}$ = 9.0 mm) and the 16*S* isomer **2** ($Z_{C38} - Z_{L1210}$ = 1.5 mm). The next steps in this evaluation involved expanding the bioassay results by including additional cancer cell lines, and this was done next.

Responses of two human solid cancer cell lines, HCT-116 and MDA-MB-435, were measured by trypane blue and the SRB method, respectively, for all 13 compounds, and the IC_{50} values are summarized in Table 5. Collectively these data showed significant inhibition for 7 of the 13 compounds and the trends against the HCT-116 cell line were somewhat similar to that observed in the disk diffusion assay. Overall, there were seven very active compounds led by **7** with the smallest IC_{50} = 0.48 μM against HCT-116. Other similarly active compounds (with HCT-116 IC_{50} values in μM) included **12** (0.92), **1** (1.1), **8** (2.1), **7a** (5.1), **9** (5.5), and **2** (7.1). The activity pattern against the MDA-MB-435 cell line was, with the exception of the response by **9** (IC_{50} > 50), almost parallel to that observed against HCT-116. The most active compound was **12** with IC_{50} = 1.0 μM. The remaining order of activity was (with IC_{50} in μM) **7** (2.1), **1** (2.8), **2** (4.8), **8** (4.0), and **7a** (7.9). While these responses are appealing, there is another important issue. Effective cytotoxins

Table 5. Bioassay Data for **1**−**12** and **7a**

compd	IC_{50} (μM)[a] HCT-116	IC_{50} (μM)[a] MDA-MB-435	ratio MDA-MB-435/HCT116	MF disrupting activity[b]
1	1.1	2.8 ± 0.3[c]	2.5	+
2	7.1	4.8 ± 0.1	0.7	+
3	38	17.0 ± 1.0	0.5	+
4	>100	34.3 ± 5.4	<0.3	−
5	49	29.7 ± 1.9	0.6	−
6	48	26.1 ± 1.0	0.5	−
7	0.48	2.1 ± 0.3	4.4	+
7a	5.1	7.9 ± 0.5	1.5	+
8	2.1	4.0 ± 0.5	1.9	+
9	5.5	>50	>9.1	−
10	>53	11.9 ± 1.1	<0.2	+
11	>53	30.5 ± 2.4	<0.6	−
12	0.92	1.0 ± 0.1	1.1	+

[a] IC_{50} values for HCT-116 and MDA-MB-435 were determined using trypane blue and SRB method, respectively. [b] The microfilament-disrupting effects were evaluated in rat aortic smooth muscle A10 cells: (+) active at 5 μM; (−) inactive at 5 μM. [c] n = 3.

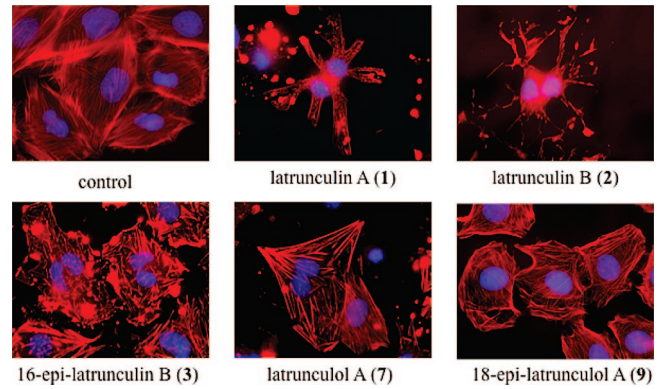

Figure 3. Microfilament disrupting effect of compounds **1**, **2**, **3**, **7**, and **9** at 5 μM against A10 cells.

such as **1** and **2** that are powerful antiactin agents are usually considered to be unsuitable for therapeutic development because of their unselective profile.[28] The IC_{50} ratios tabulated in the third column of Table 5 for the last six compounds could be interpreted as consistent with this view. Alternatively, the very different ratio computed for **9** could foreshadow a special circumstance. This possibility was investigated next.

The minilibrary was further assessed in a microfilament-disrupting assay using A10 cells.[29] Figure 3 shows the results of the phenotypic assay used, and the last column of Table 5 summarizes the level of anti-actin action at 5 μM for each of the compounds. Our results are consistent with previous studies that show, relative to the control, the expected microfilament-modulating effects exhibited by **1** and **2**. We also observed, as shown in Figure 3, significant disruption action by **3** and **7**. Analogous perturbation effects were observed (not shown here but tabulated in Table 5) for **7a**, **8**, **10**, **12** at 5 μM. By contrast, the response for **9**, while not identical to the control (Figure 3), represents the pattern expected for a compound devoid of significant microfilament-disrupting action. Similar negative responses were observed for four other compounds, **4**, **5**, **6**, and **11**. Overall, these results when evaluated side-by-side with the cytotoxicity data indicate that six of the seven very active compounds (**1**, **2**, **7**, **7a**, **8**, **12**) are aggressive actin disruptors. The different profile for **9** is intriguing, and apparently a variation in the 18*R* to 18*S* configuration of the thiazolidinone ring (**7** vs **9**) diminishes the anti-actin effect without eliminating the cytototxicity properties. This pattern does not appear to hold for the latrunculin B series, as the microfilament-disrupting

activities were similar for **2** vs **3**, in which the configuration at 16 changes from *R* to *S*.

It is worthwhile to further discuss one additional activity trend that has emerged from this study. More than 50% of the latrunuculin analogues (seven compounds) evaluated in this cell based assay study were significantly active ($IC_{50} = 0.5-10\ \mu M$) against one or both cell lines. All of these compounds possess the type 1a framework. The remaining six compounds had modest to inactive IC_{50} values, and this group included all four of the type 2 framework compounds plus two with a type 1a framework. The conformation of the 16-membered macrolide ring appears to be critical for activity as judged by the significant activity of **1**, **7**, **7a**, **8**, and **12** vs the poor responses for **10** and **11**. Not to be ignored is the requirement for the *R* configuration of the thiazolidinone ring for maximizing IC_{50} against human tumor cell lines.

Conclusions

Our findings have increased the understanding about the latrunculin family chemotypes and their cytotoxicity properties. We obtained both **1** and **2** from a Fijian *C. mycofijiensis*, which represents the first example of types 1 and 2 structures co-occurring in *Cacospongia*. The isolation and characterization of **7**−**11** possessing unprecedented new macrolide oxygenation patterns serves to further extend the record of structural information. The discovery that there are two distinct cytotoxicity modes of action operating for the latrunculin family, illustrated by the data in Table 5 for **1**, **7**, **12** vs **9**, should stimulate further interest in experimental therapeutics investigations of these compounds. The NCI database contains information about **1** (NSC 613011) and **2** (NSC 339663), but these records have been generally ignored or are unavailable to the scientific community. As another important forgotten finding, Longley demonstrated that **1** was remarkably activity against A549 lung tumor xenograft mouse model ($T/C = 146\%$).[30] This provides an important counterpoint to the observations of the DTP/NCI group that have not been able to "demonstrate a realistic therapeutic index"[28] for any cytotoxic actin inhibitor. At this juncture we have initiated efforts to further probe the preclinical potential of three new leads, **7**, **9** and **12**. The properties of **9** are especially important because they are similar to those of oxolatrunculin B,[31] as each may inhibit cancer cell line growth by an actin independent pathway.

Experimental Section

General Experimental Procedures. Optical rotations were obtained on a digital polarimeter. The NMR spectra were recorded in $CDCl_3$ and acetone-d_6 at 500 and 600 MHz for ^1H and 125.6 and 150.0 MHz for ^{13}C, respectively. Semipreparative HPLC was performed using a 5 μm C_{18} ODS column by means of a single wavelength ($\lambda = 230$ nm) for compound detection. High resolution mass measurements were obtained from an ESI-TOF mass spectrometer. DFT calculations were performed by Spartan 06 with a basis set at the B3LYP/6-31G*//B3LYP/6-31G* level. The computer used for DFT calculations was equipped with a dual 2.80 GHz CPU and 4 GB DDR2 SDRAM at 667 MHz with 222 GB disk space.

Biological Material, Collection, and Identification. Specimens of *N. magnifica*[19] (collection, no. 01600) (0.62 kg wet weight) were collected using SCUBA in 2001 off the coast of Eilat, Israel, at depths of 15 m. Two separate specimens of *C. mycofijiensis*[32] (collection nos. 00100-I and 00100-II) (1.9 and 0.6 kg wet weight) were collected using SCUBA in 2000 from the Beqa Lagoon, Fiji, at depths of 15−20 m. Taxonomic identification was based on comparison of the biological features to other samples in our repository and physical features of those previously published.[19,32] Voucher specimens and underwater photos are available.

DFT Calculations for Carbon Chemical Shifts. The carbon chemical shifts predicted by Spartan 06 were corrected by the least-squares method.[33] Score was defined by the equation [(no. of carbon − points)/(no. of carbon)] × 100 (%). The points (0−3 points) are given on the basis of the absolute difference between predicted carbon and experimental carbon chemical shift: (1) 0 points (<5 ppm), (2) 1 point (6−10 ppm), (3) 2 points (11−20 ppm), and (4) 3 points (>21 ppm).

Biological Assays. The detailed methods of the disk diffusion soft agar colony formation assay, IC_{50} determination for HCT-116 and MDA-MB-435, microfilament-disrupting assay were described previously.[34] The assay results appear in Figures 2 and 3 and Table 5.

Extraction and Isolation. Samples were preserved in the field according to our standard laboratory procedures and stored in a cold room until extraction was performed. The sponges were extracted 3× with methanol, and then the resultant oil was partitioned using a modified Kupchan-type solvent partition scheme.[35] The CH_2Cl_2 extract (FD, 180 mg) of the sponge, *N. magnifica* (collection no. 01600) was fractionated using repeated semipreparative reverse phase gradient HPLC (80:20 CH_3CN/H_2O up to 100% over 40 min) to give six fractions. Fraction H3 (7.8 mg) was then further purified using the above conditions to yield **4** (3.3 mg). Fractions H4 (51.2 mg) and H5 (11.3 mg) afforded **2** and **3**. The CH_2Cl_2 extract (FD, 75 mg) of the sponge *C. mycofijiensis* (collection no. 00100-I) was also purified using repeated semipreparative reversed-phase gradient HPLC (30:70 CH_3CN/H_2O up to 80:20 over 50 min) to give nine fractions. The resultant fractions H1−H9 eluted in the following order and afforded **10** (1.6 mg), **7** (8.3 mg), **9** (2.5 mg), **11** (2.6 mg), **8** (3.1 mg), **12** (2.8 mg), **1** (25.3 mg). Fractions H5 and H9 were not fully pursued because of limited sample size and purity. A separate purification of the lesser CH_2Cl_2 extract (00100-II FD, 75 mg) was made using the same HPLC conditions and generated 11 fractions. Additional amounts of compounds **1** and **7**−**12** were obtained along with **2** (2.2 mg).[22] These isolation procedures for the sponges *N. magnifica* (collection no. 01600) and *C. mycofijiensis* (collection no. 00100) are described in Chart S1 and S2, respectively.

Latrunculin A (1): white powder; $[\alpha]_D^{23}$ +144.4 (*c* 1.0, $CHCl_3$); ^1H and ^{13}C NMR data in Table S1; HRESITOFMS *m/z* 444.1827 $[M + Na]^+$ (calcd for $C_{22}H_{31}NO_5SNa$ 444.1815). This compound was identified by comparison of spectral data with those of the literature values.[22]

Latrunculin B (2): white powder; $[\alpha]_D^{23}$ +120.1 (*c* 4.0, $CHCl_3$); ^1H and ^{13}C NMR data in Table S2; HRESITOFMS *m/z* 418.1653 $[M + Na]^+$ (calcd for $C_{20}H_{29}NO_5SNa$ 418.1659). This compound was identified by comparison of spectral data with those of the literature values.[22]

16-*epi*-Latrunculin B (3): white powder; $[\alpha]_D^{23}$ + 81.2 (*c* 1.0, $CHCl_3$); ^1H and ^{13}C NMR data in Table S3; HRESITOFMS *m/z* 418.1649 $[M + Na]^+$ (calcd for $C_{20}H_{29}NO_5SNa$ 418.1659). This compound was identified by comparison of spectral data with those of the literature values.[8]

Latrunculin C (4): white powder; ^1H and ^{13}C NMR in Table S4; HRESITOFMS *m/z* 420.1815 $[M + Na]^+$ (calcd for $C_{20}H_{31}NO_5SNa$ 420.1798). This compound was identified by comparison of spectral data with those of the literature values.[18]

Library Compounds. 15-Methoxylatrunculin B (**5**) and latrunculeic acid (**6**) were used for the disk diffusion cell-based assay. The purity (>95%) for **5** and **6** was confirmed by LCMS and ^1H NMR analysis.[19,36]

Latrunculol A (7): white powder; $[\alpha]_D^{26}$ +64.8 (*c* 5.6, MeOH); UV (MeOH) λ_{max} (log ε) 216 nm (4.07); ^1H and ^{13}C NMR data in Tables 2, 3, and S5; HRESITOFMS *m/z* 478.1864 $[M + Na]^+$ (calcd for $C_{22}H_{33}NO_7SNa$ 478.1870).

Formation of Acetonide 7a from 7. To a solution of **7** (5.0 mg) in CH_2Cl_2 (0.5 mL) were added 2,2-dimethoxypropane (0.75 mL) and pyridinium toluene *p*-sulfonate (9.0 mg). After stirring of

the mixture at room temperature for 2 h, the solvent was evaporated under reduced pressure. The residue was purified by HPLC using acetonitrile−water (1:1 to 1:0) as the eluent to afford acetonide **7a** (2.5 mg) as a colorless powder.

Acetonide 7a: colorless powder; $[\alpha]_D^{28}$ +21.7 (*c* 1.7, MeOH); ^{1}H NMR δ ppm ($CDCl_3$) 5.70 (1H, d, J = 1.4 Hz, H-2), 5.64 (1H, br s, NH), 5.44 (1H, dd, J = 10.7 and 9.6 Hz, H-9), 5.39 (1H, dd, J = 10.8 and 8.7 Hz, H-8), 5.38 (1H, m, H-15), 4.45 (1H, t, J = 8.5 Hz, H-7), 4.05 (1H, br t, 9.8 Hz, H-13), 3.83 (1H, ddd, J = 8.8, 5.6, and 1.0 Hz, H-18), 3.77 (1H, ddd, J = 8.6, 5.9 and 4.3 Hz, H-6), 3.50 (1H, dd, J = 11.6, 8.9 Hz, H-19b), 3.41 (1H, dd, J = 11.6 and 6.0 Hz, H-19a), 2.55−2.63 (3H, m, H_2-4 and H-10), 2.08 (1H, dt, J = 14.6 and 2.2 Hz, H-16b), 1.95 (3H, s, H_3-21), 1.90 (1H, br d, J = 14.6 Hz, H-16a), 1.67−1.76 (5H, m, H_2-5, H-11b and H-14b), 1.40−1.56 (3H, m, H_2-12, H-14a), 1.44 (3H, s, H_3-acetonide), 1.43 (3H, s, H_3-acetonide), 1.20 (1H, m, H-11a), 1.02 (3H, d, J = 5.5 Hz, H_3-22); NOESY 1D (mixing time = 0.5 ms) H-8/H-6, H-7/H-10; HRESIMS *m/z* 518.2178 $[M + Na]^+$ (calcd for 518.2183, $C_{25}H_{37}NO_7SNa$).

Latrunculol B (8): white powder; $[\alpha]_D^{27}$ +47.5 (*c* 1.6, MeOH); UV (MeOH) λ_{max} (log ε) 216 nm (3.95); ^{1}H and ^{13}C NMR data in Tables 2, 3, and S7. HRESITOFMS *m/z* 492.2025 $[M + Na]^+$ (calcd for $C_{23}H_{35}NO_7SNa$ 492.2027).

18-*epi*-Latrunculol A (9): white powder; $[\alpha]_D^{27}$ +55.2 (*c* 4.4, MeOH); UV (MeOH) λ_{max} (log ε) 216 nm (4.06); ^{1}H and ^{13}C NMR data in Figures S15 and S16, and Table S8; HRESITOFMS *m/z* 478.1866 $[M + Na]^+$ (calcd for $C_{22}H_{33}NO_7SNa$ 478.1870).

Latrunculol C (10): white powder; $[\alpha]_D^{28}$ +56.1 (*c* 1.3, MeOH); UV (MeOH) λ_{max} (log ε) 216 nm (4.50); ^{1}H and ^{13}C NMR data in Tables 2, 3, and S9; HRESITOFMS *m/z* 478.1878 $[M + Na]^+$ (calcd for $C_{22}H_{33}NO_7SNa$ 478.1870).

Latrunculone A (11): white powder; $[\alpha]_D^{27}$ +5.8 (*c* 1.2, MeOH); UV (MeOH) λ_{max} (log ε) 216 nm (4.23); ^{1}H and ^{13}C NMR data in Tables 2, 3, and S10; HRESITOFMS *m/z* 476.1707 $[M + Na]^+$ (calcd for $C_{22}H_{31}NO_7SNa$ 476.1714).

Latrunculone B (12): white powder; $[\alpha]_D^{29}$ +129.2 (*c* 0.1, MeOH); ^{1}H and ^{13}C NMR data in Tables 2, 3, and S11; HRESITOFMS *m/z* 460.1764 $[M + Na]^+$ (calcd for $C_{22}H_{31}NO_6SNa$ 460.1735).

Acknowledgment. This work was supported by the National Institutes of Health Grant R01 CA 47135, NMR equipment Grants NSFCHE-0342912 and NIH S10-RR19918, MS equipment Grant NIH S10-RR20939, and funding from the Joe and Jessie Crump Foundation (S.L.M.). We thank C. P. Loo and D. B. Cordes for the initial isolation work of *C. mycofijiensis*. We also thank D. LaBoeuf for her excellent technical assistant. We thank M. Ilan and the members of the Ilan Research Group for their generous assistance in the permit acquisition and collection of *N. magnifica*. We are also grateful to W. Aalbersberg, University of the South Pacific, Fiji, and A. Raiwalui, Permanent Secretary for the Director of Fisheries, Ministry of Agriculture, Fisheries and Forests Division, for obtaining administrative approvals to carry out research in Fiji.

Supporting Information Available: Isolation scheme and underwater picture for *N. magnifica* and *C. mycofijiensis*, NMR data for **1**−**4** and **7**−**12**, and DFT calculations results for **7** and **10**. This material is available free of charge via the Internet at http://pubs.acs.org.

References

(1) Kashman, Y.; Groweiss, A.; Shmueli, U. Latrunculin, a New 2-Thiazolidinone Macrolide from the Marine Sponge *Latrunculia magnifica*. *Tetrahedron Lett.* **1980**, *21*, 3629–3632.
(2) Spector, I.; Shochet, N. R.; Kashman, Y.; Groweiss, A. Latrunculins: Novel Marine Toxins That Disrupt Microfilament Organization in Cultured Cells. *Science* **1983**, *219*, 493–495.
(3) Sonnenschein, R. N.; Johnson, T. A.; Tenney, K.; Valeriote, F. A.; Crews, P. A Reassignment of (−)-Mycothiazole and the Isolation of a Related Diol. *J. Nat. Prod.* **2006**, *69*, 145–147.
(4) Gerth, K.; Bedorf, N.; Hoefle, G.; Irschik, H.; Reichenbach, H. Antibiotics from Gliding Bacteria. 74. Epothilons A and B: Antifungal and Cytotoxic Compounds from *Sorangium cellulosum* (Myxobacteria): Production, Physico-Chemical and Biological Properties. *J. Antibiot.* **1996**, *49*, 560–563.
(5) Hoefle, G.; Bedorf, N.; Steinmetz, H.; Schomburg, D.; Gerth, K.; Reichenbach, H. Antibiotics from Gliding Bacteria. 77. Epothilone A and B. Novel 16-Membered Macrolides with Cytotoxic Activity: Isolation, Crystal Structure, and Conformation in Solution. *Angew. Chem., Int. Ed. Engl.* **1996**, *35*, 1567–1569.
(6) Coue, M.; Brenner, S. L.; Spector, I.; Korn, E. D. Inhibition of Actin Polymerization by Latrunculin A. *FEBS Lett.* **1987**, *213*, 316–318.
(7) Hayot, C.; Debeir, O.; Van Ham, P.; Van Damme, M.; Kiss, R.; Decaestecker, C. Characterization of the Activities of Actin-Affecting Drugs on Tumor Cell Migration. *Toxicol. Appl. Pharmacol.* **2006**, *211*, 30–40.
(8) Hoye, T. R.; Ayyad, S.-E. N.; Eklov, B. M.; Hashish, N. E.; Shier, W. T.; El Sayed, K. A.; Hamann, M. T. Toward Computing Relative Configurations: 16-*epi*-Latrunculin B, a New Stereoisomer of the Actin Polymerization Inhibitor Latrunculin B. *J. Am. Chem. Soc.* **2002**, *124*, 7405–7410.
(9) Ayscough, K. R.; Stryker, J.; Pokala, N.; Sanders, M.; Crews, P.; Drubin, D. G. High Rates of Actin Filament Turnover in Budding Yeast and Roles for Actin in Establishment and Maintenance of Cell Polarity Revealed Using the Actin Inhibitor Latrunculin-A. *J. Cell Biol.* **1997**, *137*, 399–416.
(10) Morton, W. M.; Ayscough, K. R.; McLaughlin, P. J. Latrunculin Alters the Actin−Monomer Subunit Interface To Prevent Polymerization. *Nat. Cell Biol.* **2000**, *2*, 376–378.
(11) Furstner, A.; De Souza, D.; Parra-Rapado, L.; Jensen, J. T. Catalysis-Based Total Synthesis of Latrunculin B. *Angew. Chem., Int. Ed.* **2003**, *42*, 5358–5360.
(12) White, J. D.; Kawasaki, M. Total Synthesis of (+)-Latrunculin A, an Ichthyotoxic Metabolite of the Sponge *Latrunculia magnifica* and Its C-15 Epimer. *J. Org. Chem.* **1992**, *57*, 5292–5300.
(13) White, J. D.; Kawasaki, M. Total Synthesis of (+)-Latrunculin A. *J. Am. Chem. Soc.* **1990**, *112*, 4991–4993.
(14) Smith, A. B., III; Noda, I.; Remiszewski, S. W.; Liverton, N. J.; Zibuck, R. Total Synthesis of (+)-Latrunculin A. *J. Org. Chem.* **1990**, *55*, 3977–3979.
(15) Zibuck, R.; Liverton, N. J.; Smith, A. B., III. Total Synthesis of (+)-Latrunculin B. *J. Am. Chem. Soc.* **1986**, *108*, 2451–2453.
(16) Fuerstner, A.; De Souza, D.; Turet, L.; Fenster, M. D. B.; Parra-Rapado, L.; Wirtz, C.; Myott, R.; Lehmann, C. W. Total Syntheses of the Actin-Binding Macrolides Latrunculin A, B, C, M, S and 16-*epi*-Latrunculin B. *Chem.−Eur. J.* **2006**, *13*, 115–134.
(17) Kakou, Y.; Crews, P.; Bakus, G. J. Dendrolasin and Latrunculin A from the Fijian Sponge *Spongia mycofijiensis* and an Associated Nudibranch *Chromodoris lochi*. *J. Nat. Prod.* **1987**, *50*, 482–484.
(18) Kashman, Y.; Groweiss, A.; Lidor, R.; Blasberger, D.; Carmely, S. Latrunculins: NMR Study, Two New Toxins and a Synthetic Approach. *Tetrahedron* **1985**, *41*, 1905–1914.
(19) Vilozny, B.; Amagata, T.; Mooberry, S. L.; Crews, P. A New Dimension to the Biosynthetic Products Isolated from the Sponge *Negombata magnifica*. *J. Nat. Prod.* **2004**, *67*, 1055–1057.
(20) Crews, P.; Kakou, Y.; Quinoa, E. Mycothiazole, a Polyketide Heterocycle from a Marine Sponge. *J. Am. Chem. Soc.* **1988**, *110*, 4365–4368.
(21) Johnson, T. A.; Amagata, T.; Oliver, A. G.; White, K. N.; Tenney, K.; Valeriote, F. A.; Crews, P. The unexpected isolation of CTP-431, a novel thiopyrone from the sponge *Cacospongia mycofijiensis*. *J. Org. Chem.* **2008**, *73*, 7255–7259.
(22) Groweiss, A.; Shmueli, U.; Kashman, Y. Marine Toxins of *Latrunculia magnifica*. *J. Org. Chem.* **1983**, *48*, 3512–3516.
(23) Nagle, D. G.; Gerwick, W. H. Structure and Stereochemistry of Constanolactones A−G, Lactonized Cyclopropyl Oxylipins from the Red Marine Alga *Constantinea simplex*. *J. Org. Chem.* **1994**, *59*, 7227–7237.
(24) *Spartan 06*; Wavefunction, Inc.: Irvine, CA; http://www.wavefun.com.
(25) Amagata, T.; White, K. N.; Wenzel, P. J.; Crews, P. Unpublished results.
(26) Jefford, C. W.; Bernardinelli, G.; Tanaka, J.; Higa, T. Structures and Absolute Configurations of the Marine Toxins, Latrunculin A and Laulimalide. *Tetrahedron Lett.* **1996**, *37*, 159–162.
(27) Valeriote, F.; Grieshaber Charles, K.; Media, J.; Pietraszkewicz, H.; Hoffmann, J.; Pan, M.; McLaughlin, S. Discovery and Development of Anticancer Agents from Plants. *J. Exp. Ther. Oncol.* **2002**, *2*, 228–236.
(28) Newman, D. J.; Cragg, G. M. Marine Natural Products and Related Compounds in Clinical and Advanced Preclinical Trials. *J. Nat. Prod.* **2004**, *67*, 1216–1238.

(29) Mooberry, S. L.; Tien, G.; Hernandez, A. H.; Plubrukarn, A.; Davidson, B. S. Laulimalide and Isolaulimalide, New Paclitaxel-Like Microtubule-Stabilizing Agents. *Cancer Res.* **1999**, *59*, 653–660.

(30) Longley, R. E.; McConnell, O. J.; Essich, E.; Harmody, D. Evaluation of Marine Sponge Metabolites for Cytotoxicity and Signal Transduction Activity. *J. Nat. Prod.* **1993**, *56*, 915–920.

(31) Ahmed, S. A.; Odde, S.; Daga, P. R.; Bowling, J. J.; Mesbah, M. K.; Youssef, D. T.; Khalifa, S. I.; Doerksen, R. J.; Hamann, M. T. Latrunculin with a Highly Oxidized Thiazolidinone Ring: Structure Assignment and Actin Docking. *Org. Lett.* **2007**, *9*, 4773–4776.

(32) Sanders, M. L.; van Soest, R. W. M. A Revised Classification of *Spongia mycofijiensis*. In *Recent Advances in Sponge Biodiversity Inventory and Documentation*; Willenz, P., Ed.; Bulletin de l'Institut Royal Sciences Naturelles de Belgique, Biologie, Suppl., Vol. 66; Institut Roayl des Scineces Naturelle de Belgique: Brussels, Belgium, 1996; pp 117−122.

(33) Rychnovsky, S. D. Predicting NMR Spectra by Computational Methods: Structure Revision of Hexacyclinol. *Org. Lett.* **2006**, *8*, 2895–2898.

(34) Johnson, T. A.; Tenney, K.; Cichewicz, R. H.; Morinaka, B. I.; White, K. N.; Amagata, T.; Subramanian, B.; Media, J.; Mooberry, S. L.; Valeriote, F. A.; Crews, P. Sponge-Derived Fijianolide Polyketide Class: Further Evaluation of Their Structural and Cytotoxicity Properties. *J. Med. Chem.* **2007**, *50*, 3795–3803.

(35) Thale, Z.; Johnson, T.; Tenney, K.; Wenzel, P. J.; Lobkovsky, E.; Clardy, J.; Media, J.; Pietraszkiewicz, H.; Valeriote, F. A.; Crews, P. Structures and Cytotoxic Properties of Sponge-Derived Bisannulated Acridines. *J. Org. Chem.* **2002**, *67*, 9384–9391.

(36) Blasberger, D.; Carmely, S.; Cojocaru, M.; Spector, I.; Shochet, N. R.; Kashman, Y. On the Chemistry of Latrunculins A and B. *Liebigs Ann. Chem.* **1989**, *117*, 1–1188.

JM8008585